

Enhancing the Washing Durability and Electrical Longevity of Conductive Polyaniline-Grafted Polyester Fabrics

Muhammad Faiz Aizamddin and Mohd Muzamir Mahat*

Cite This: *ACS Omega* 2023, 8, 37936–37947

Read Online

ACCESS |



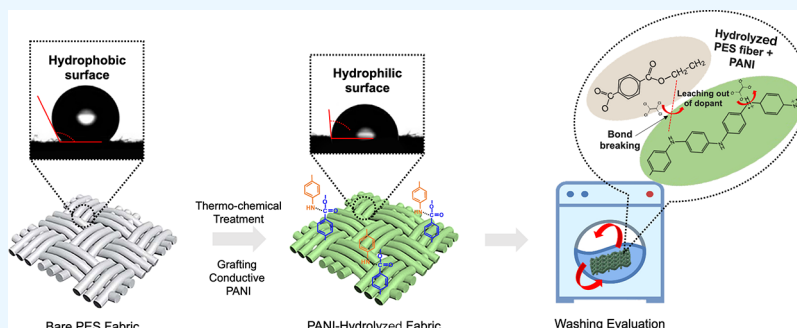
Metrics & More



Article Recommendations



Supporting Information



ABSTRACT: The demand for wearable electronics has driven the development of conductive fabrics, particularly those incorporating polyaniline (PANI) that is known for its high electrical conductivity, flexibility, and ease of fabrication. However, the limited stability and durability of the conductive fabric, especially during washing, present significant challenges. The drawbacks can be traced by weak physical attachment between the fabric and the conductive coating, leading to a decrease in conductivity over time. These drawbacks significantly impact the fabric's functionality and performance, highlighting the need for effective solutions to enhance its stability and durability. This study focuses on addressing these challenges by employing a thermochemical treatment. A hydrophilic surface of the polyester fabric is obtained after the treatment (hydrolysis), followed by grafting of PANI on it. The adhesion between PANI and the polyester fabrics was found to be enhanced, as proved by contact angle analysis. Furthermore, the PANI-hydrolyzed fabrics (treated) demonstrated stable conductivity ($\sim 10^{-3} \text{ S cm}^{-3}$) even after 10 washing cycles, showcasing their excellent durability. In comparison, the unhydrolyzed PANI fabric experienced a drop in conductivity by three orders of magnitude. X-ray photoelectron spectroscopy via $N 1s$ core line spectra showed chemical shifts and quantified the level of doping through PANI's protonation level. We found that PANI-hydrolyzed fabrics preserved their dedoping level from 44.77 to 42.68%, indicating improved stability and extension of their electrical properties' lifetime after washing as compared to unhydrolyzed (untreated) fabrics, from 36.99 to 26.61%. This investigation demonstrates that the thermochemical approach can effectively enhance the durability of conductive PANI fabrics, enabling them to withstand the washing process while preserving their electrical endurance.

INTRODUCTION

Conductive fabrics are integral components in various devices, including pressure sensors, antennas, electromagnetic interference (EMI) shielding devices, flexible heaters, and static control clothing. These fabrics possess specific electrical properties that enable their effective utilization in a diverse range of applications.^{1–5} Furthermore, this fabric class is critical in next-generation wearable consumer electronics and smart clothing.^{6,7} The hybrid of intelligent functionality and flexibility of fashionable clothing forms the foundation of innovative applications in military, public safety, healthcare, sports, and consumer fitness. Generally, a conductive fabric can be created by weaving metal strands into the fabric. Other alternatives include coating (depositing) or embedding conductive components, such as carbon, nickel, copper, gold, silver, or titanium on the fabric.⁸ Although these composite fabrics have excellent conductivities, they are not without

limitations. Stiffness and ease of degradation, which may be caused by wire breakage, sloughing of depositions, or chemical corrosion during an active application, are some of the flaws associated with composite fabrics.⁶

Conductive polymers (CPs) have emerged as a promising alternative to address the challenges. They have garnered significant attention due to their ability to exhibit excellent electrical, magnetic, and optical properties, comparable to those commonly associated with metals.^{9–13} In addition, CPs carry the qualities of lightweight, flexibility, and simple

Received: May 15, 2023

Accepted: July 18, 2023

Published: October 3, 2023



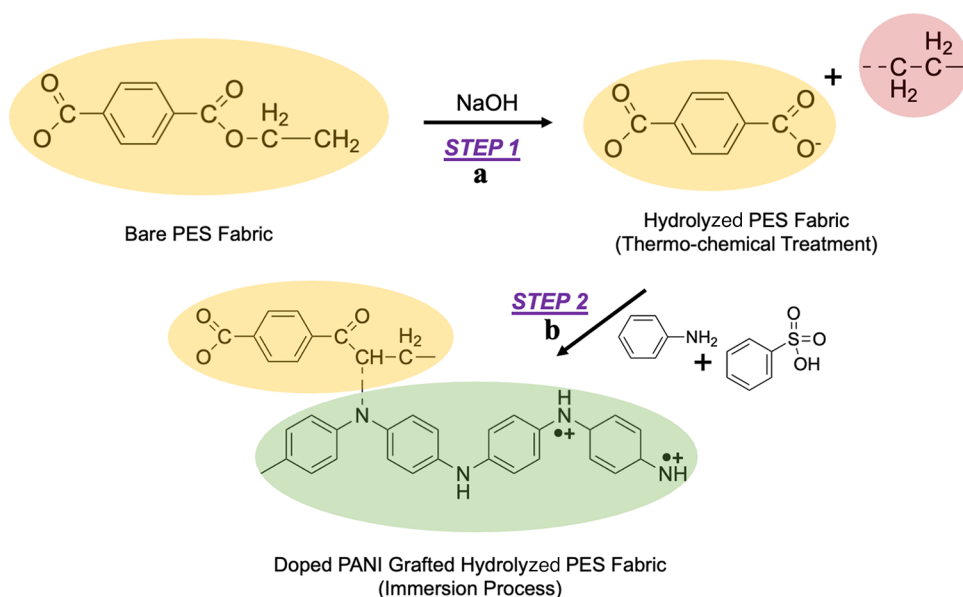


Figure 1. Preparation of conductive PANI fabrics through thermochemical treatment. (a) *Step 1*: Partial removal of the hydroxyl end group from the ester group in PES fibers through thermochemical treatment. (b) *Step 2*: Doped PANI solution from a previous study was grafted onto hydrolyzed PES fabrics via immersion.

processability.¹⁴ Polyaniline (PANI) has piqued the interest of researchers due to its lightness, excellent environmental and thermal stability, high electrical conductivity, good optical properties, ease of manufacture, and affordability. Furthermore, the conductivity of PANI can be modified by manipulating its oxidation state and protonation level.^{10,15} This freedom of manipulation makes it an excellent alternative for constructing multifunctional conductive materials. Due to its soft nature, depositing PANI onto fabric substrates is a viable technique to address the stiffness and chemical corrosion associated with typical metal/fabric blends. However, weak durability upon washing is a major hurdle in fabric blends due to the leaching of PANI and the conductive agent from the fabric.^{16,17} In practice, fabric materials inevitably accumulate dirt, dust, and stains, emphasizing the importance of washing to maintain cleanliness and hygiene. In the case of PANI fabrics, proper washing is essential not only for removing contaminants but also for preserving the fabric's appearance and extending its lifespan. However, the mechanical scrubbing and chemical soaking involved in the washing process can potentially damage the coatings on the conductive layers, further jeopardizing the fabric's electrical integrity.^{18,19} Therefore, it is necessary to improve the durability and lifespan of PANI fabrics while preserving their electrical integrity.

Polyethylene terephthalate or polyester (PES) fabrics are widely utilized as the base material in clothing, sportswear, packaging, smart electronic, and furniture materials.²⁰ PES fabrics have a range of advantages, which are lightweight, high tensile strength, flexibility, quick-drying, reduced wrinkles and shrinkage rates, excellent thermal and chemical stability, good dimensional stability, resistance to environmental stimulus, and low-cost production.²¹ However, due to their inert molecular structure and low moisture absorption rate, they have low hydrophilicity and poor adhesion to conductive coatings like PANI.²² Therefore, it is necessary to introduce chemical and physical changes to PES fabrics. These changes aim to maximize the holding capability of PANI within the fabric while extending the durability of its electrical functionalities.

Various chemical treatments, including acid treatment, aminolysis, and graft polymerization, have been employed to modify the hydrophilicity of PES fabrics, thereby altering their texture drape, dyeing depth, and strength. However, these approaches have obstacles, such as degradations of the bulk and mechanical properties of the PES fabric, require high energy consumption, and possess environmental contamination.²³

Alkaline hydrolysis is a technique to introduce hydrophilicity to PES fabrics. According to Musale and Shukla, PES could be nucleophilically substituted and hydrolyzed by aqueous sodium hydroxide.²⁴ The hydroxyl ions attacked the polyester's electron-deficient carbonyl carbons to create an intermediate anion. This action increased the number of hydrophilic groups on the fiber surface. The nucleophilic assault of NaOH on PES chains generated chain scissions at the ester linkages, resulting in carboxyl and hydroxyl polar groups. These polar groups improved the polarity and hydrogen bonding with water molecules, resulting in greater wettability on the hydrolyzed fabric.²⁵ Due to the covalent connection between PANI and the fabric, the grafting modification of polymer substrates is a reliable technique for fabricating stable, functional materials.²⁶

This paper explores the grafting of PANI onto hydrolyzed PES fabrics, producing an enhanced stability and durability of the conductive fabrics when exposed to washing. A bare PES fabric was first subjected to a thermochemical treatment, modifying its surface hydrophilicity, followed by grafting of PANI onto the fabric via immersion. The individual steps to prepare conductive PANI in this investigation are depicted in Figure 1. This approach is aimed to eliminate the drawback of PANI insolubility while simultaneously improving the surface adhesion of grafted PANI on the fabric. This study includes the evaluation of the washing durability of the PANI fabric, such as the measurement of electrical conductivity, protonation level, and its hydrophilicity properties.

■ EXPERIMENTAL SECTION

Materials. A 50 × 50 cm² bare polyester fabric was purchased from Kamdar Sdn. Bhd. (Klang, Malaysia). Aniline solution, sodium hydroxide (NaOH), *para*-toluene sulfonic acid (*p*TSA), and dimethyl sulfoxide (DMSO) (reagent plus, 99%) were purchased from Sigma-Aldrich (St. Louis, MO, USA). Tetrachloroethylene (TTE) was sourced from System, (Shah Alam, Malaysia).

Preparation of Hydrolyzed PES Fabric via Thermochemical Treatment. The overall procedure of thermochemical treatment of the PES fabric is illustrated in Figure S1. In the pretreatment process, the PES fabrics were rinsed in acetone and dried for 30 min. The bare PES fabric (each weighing 1.8 g) was subjected to alkaline NaOH with various concentrations (3, 6, 9, 12, 15, 18, and 21 wt %) at 80 °C. The treatment time of 90 min was used for this evaluation since it could maximize the water absorption rate as optimized in Figure S2. The treatment in 12 wt % NaOH for 90 min achieved the maximum water absorption rate. Subsequently, the hydrolyzed fabrics were neutralized with 5 mL of acetic acid (50–60 °C) and rinsed with distilled water to remove residual NaOH. In the final stage, a hot rinsing with distilled water was performed until a pH of 7 was registered (verified through filter paper) and dried at room temperature (25–27 °C).

Fabrication of Hydrolyzed PANI PES Fabrics. The fabrication of conductive PANI fabrics was accomplished with the immersion technique, as described in the previous study.^{27–30} Bare PES fabrics with a size of 5 × 5 cm² were immersed in 15 mL of PANI solution. The fabrics were soaked for 30 min at room temperature. The fabrics were dried at room temperature for 24 h and stored under dark conditions. The immersion process is illustrated in Figure S3.

Degree of Grafting of PANI onto Hydrolyzed PES Fabrics. Chemical grafting is the attachment or absorption of polymer chains to the substrate surface.³¹ The diffusion of PANI molecules in solution on the fabric substrate is critical to accomplish the required degree of grafting (DG) of PANI, which imparts its electrical network.^{18,32} The hydrolyzed fabrics were immersed in 15 mL of conductive PANI solution. The fabrics were soaked for 30 min and dried at room temperature for 24 h. Similar procedures were repeated for different concentrations of hydrolyzed PES fabrics onto PANI solutions. The DG of PANI was calculated according to eq 1:

$$\text{DG of PANI (\%)} = (W_{\text{after}} - W_{\text{before}}) / W_{\text{after}} \times 100 \quad (1)$$

where W_{after} is the weight of the hydrolyzed fabric after grafting with PANI and W_{before} is the weight of the hydrolyzed fabric.

Washing Durability Evaluation. The combination of 132-2004 and 86-2005 procedures (recommended by the American Association of Textile Chemists and Colorists) was simplified to study the durability of the fabrics. The 5 × 5 cm² PANI fabrics (hydrolyzed and nonhydrolyzed) were sewn at all four edges to ensure consistent test results over the surface. The fabrics were immersed in 200 mL of TTE detergent solution and agitated for 30 min at 60 °C in metal-capped bottles. The treated fabrics were dried at 20 °C in a ventilated hood for an hour before being subjected to the characterizations. A similar process was repeated for 10 cycles. The electrical measurements of the treated fabrics were performed in each cycle. The schematic diagram of the washing evaluation of PANI fabrics is illustrated in Figure S4.

Material Characterization. The structural and intermolecular interactions of the samples were studied with PerkinElmer Spectrum 100 attenuated total reflectance-Fourier transform infrared (ATR-FTIR) spectroscopy. The analysis was performed at room temperature with ambient humidity. The spectra were recorded from 600 to 1500 cm⁻¹ at 20 kHz frequency with a resolution of 16 cm⁻¹. Each spectrum was recorded with a mirrored diamond surface under spectroscopic circumstances. The spectrum was analyzed with Bio-Rad Win-IR Pro software (version 10, PerkinElmer Ltd., London, United Kingdom) to identify the functional groups within the fabricated fabrics. The electrical conductivity of PANI fabrics was measured with electrochemical impedance spectroscopy (EIS) (model: HIOKI 3532-50 LCR Hi-TESTER, HIOKI E. E. Corporation, Nagano, Japan). The analysis was performed at room temperature with a frequency range of 100 Hz to 1000 kHz. The 5 × 5 cm² hydrolyzed PANI fabrics were clamped between two copper electrodes with a 1 cm diameter. The measurement was repeated three times to obtain an average value. The conductivity was derived from the following eq 2:³³

$$\sigma = L / (R_b \times A) \quad (2)$$

where σ is conductivity, R_b is the bulk resistance measured by the instrument, L is the sample thickness, and A is the cross-sectional area of the electrode. The morphological and elemental distribution of the samples were observed with scanning electron microscopy (SEM) (SNE-4500 M Plus Tabletop SEM, SEC Co., Ltd., Suwon-si, South Korea) and energy dispersive X-ray (EDX) mapping analysis, respectively. A 0.5 × 0.5 cm² fabric sample was mounted on the sample stage with carbon tape and placed in a sample chamber. All fabrics were gold-sputtered to improve image resolution. A magnification range from 300× to 1000× was employed. The fabric's mechanical strength was analyzed with a universal strength tester machine (Tenso Lab 5000, MESDAN S.P.A, Puegnago del Garda (BS)-Italy). The test complied with the ASTM D5035-95 protocol. The 20 × 7.5 cm² fabrics were prepared and tested in warp and weft structures. A 300 mm/min transverse rate and 5 kN load force were applied for each sample. Tensile strength and percentage elongation at break were recorded. X-ray photoelectron spectroscopy (XPS) analysis was performed with Thermo Fisher Scientific (model = Nexsa G2 XPS) with a monochromatic Al-K α X-ray source of 1486.6 eV. The operating parameters were fixed at 3 mA and 15 kV to analyze an area of 100 μ m diameter under a 4.8 × 10⁻⁷ mBar ultrahigh vacuum environment. A narrow scan was performed at a step size of 0.1 eV with a multichannel detector. The analyzer was operated in a fixed transmission mode with a pass energy of the hemispherical analyzer at 100 eV for high-resolution scans/narrow scans with a minimum cycle of 20 times. All scans were performed under charge neutralization with a low-energy electron gun within the magnetic field lens. The spectra were analyzed (deconvoluted) with Avantage software and Shirley background. Survey spectra in the range of 0 to 900 eV were recorded for each sample, followed by high-resolution measurement line spectra for C 1s, N 1s, and S 2p core levels. The binding energy scale was calibrated with reference to the C 1s line at 285 eV. The amine peak was fixed at 400 eV, while the peaks for imine, protonated amine, and protonated imine were defined at 398, 400, and 402 eV, respectively. The changes in the fabrics' doping level were calculated from the ratio of N⁺/N_{total}. The treated fabrics (dry) were weighed at 1.8 g. The fabrics were immersed in 30

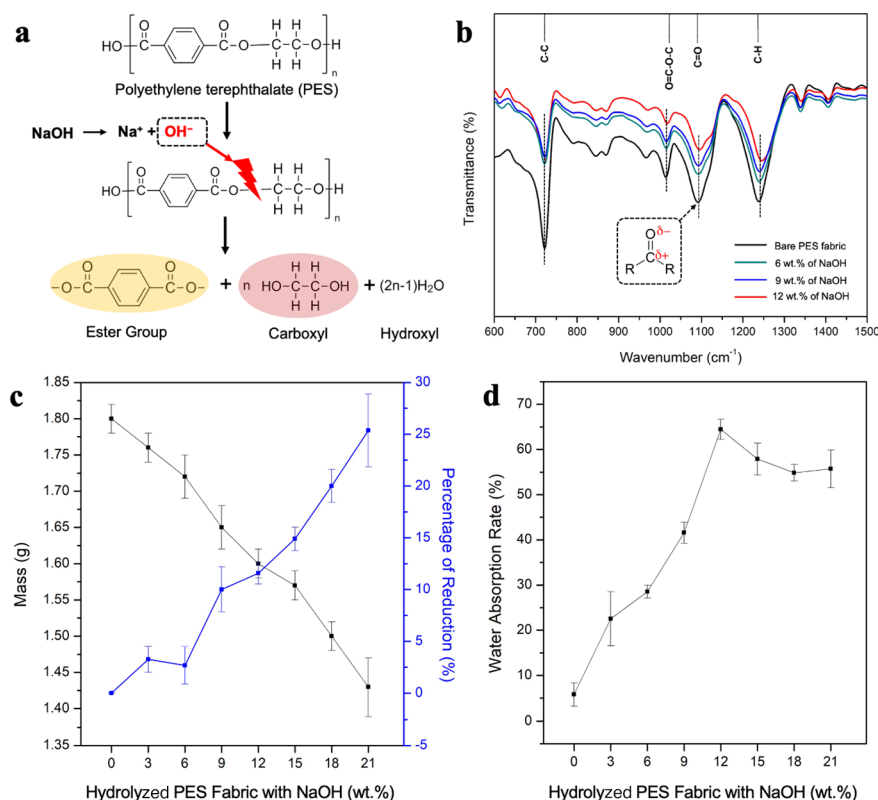


Figure 2. (a) Proposed mechanism of bond breaking in PES fabrics during hydrolysis. (b) IR spectra of hydrolyzed PES fabrics in various NaOH concentrations. (c) Effects of different NaOH concentrations on weight variations and the corresponding percentage on the weight loss of fabrics. (d) Effect of hydrolyzed PES fabrics with various NaOH concentrations on the water absorption rate.

mL of distilled water at room temperature for 5 min. The fabrics were promptly hung until all water droplets had evaporated from them. Next, the wet fabrics were weighted with a precise digital balance machine (model: Balance XPR226DR, METTLER TOLEDO, Switzerland). Equation 3 was employed to calculate the water absorption rate:

$$\text{water absorption rate (\%)} = (W_w - D_w) / (D_w) \times 100 \quad (3)$$

where W_w is the weight of the wet fabric and D_w is the weight of the dried treated fabric. A contact angle tester, Theta Lite Optical Tensiometer (Contact Angle Meter, Phoenix, USA), was utilized to test the water contact angle of the bare and treated fabrics. Distilled water droplets with a volume of 3 μL were placed on the fabrics with a microliter syringe. Each contact angle value represented a minimum of five measurements at various positions on the fabrics.

RESULTS AND DISCUSSION

PES hydrolysis via thermochemical treatment was initiated by hydroxyl ions from NaOH that attacked electron-deficient carbonyl carbons, e.g., C=C, C-O, C-O-C of the PES chains to form an intermediate anion.³⁴ The reaction rate sped up when the temperature reached 60 °C.³⁵ This condition led to partial removal of a low molecular segment of the chains like carboxyl, which resulted in weight loss of the fabric. The extent of the attack and removal of short-chain segments increased linearly with NaOH concentration. Simultaneously, a surge in -COOH and -OH hydrophilic groups was introduced to ester components.³⁶ The proposed mechanism of bond

breaking in PES fabrics during hydrolysis is illustrated in Figure 2a.

The infrared (IR) spectra in Figure 2b reflect the chemical structure in the hydrolyzed fabrics. The peak at 1100 cm⁻¹ suggested C=O stretching vibration, which was a characteristic of the carbonyl group (C=O) in PES.³⁷ Upon increasing of alkaline concentration, a plunge in intensity of C=O was recorded. This condition possibly affected the absorption rate since the carbonyl group was a polar group that attracted water.³⁸ Evidence of alkaline hydrolysis on PES fabrics was shown by the drop in the peak at 1249 and 1012 cm⁻¹. This observation reflected the elimination of short chains in the ester linkage.³⁹ Simultaneously, the peaks at 725.32 cm⁻¹ were attributed to the carbon-carbon chain of the carboxylic group on the fabric's surface.⁴⁰

The hydrolysis of PES showed a significant weight loss of 25.36% when the NaOH concentration was raised to 21 wt %, as seen in Figure 2c. According to a past study, a weight loss from 15 to 30% could contribute to overall depreciation in stiffness, tenacity, and elongation of PES fabrics.²⁵ A recent study showed that PES fabrics experienced a significant weight loss when hydrolyzed.⁴¹ However, the extent of weight loss depends on hydrolytic conditions and utilized agents.⁴² This agreement denotes that oxidizing agents, such as NaOH, have a redox impact on the PES fiber surface. This redox reaction can transform its physical properties, such as tensile strength, elongation, and physical structure.

The water absorption by the fiber leads to swelling of the material, dimensional changes, reduction in rigidity, and poor strength and stiffness.^{43,44} In this study, there was a steady increase in the water absorption rate by the hydrolyzed fabrics

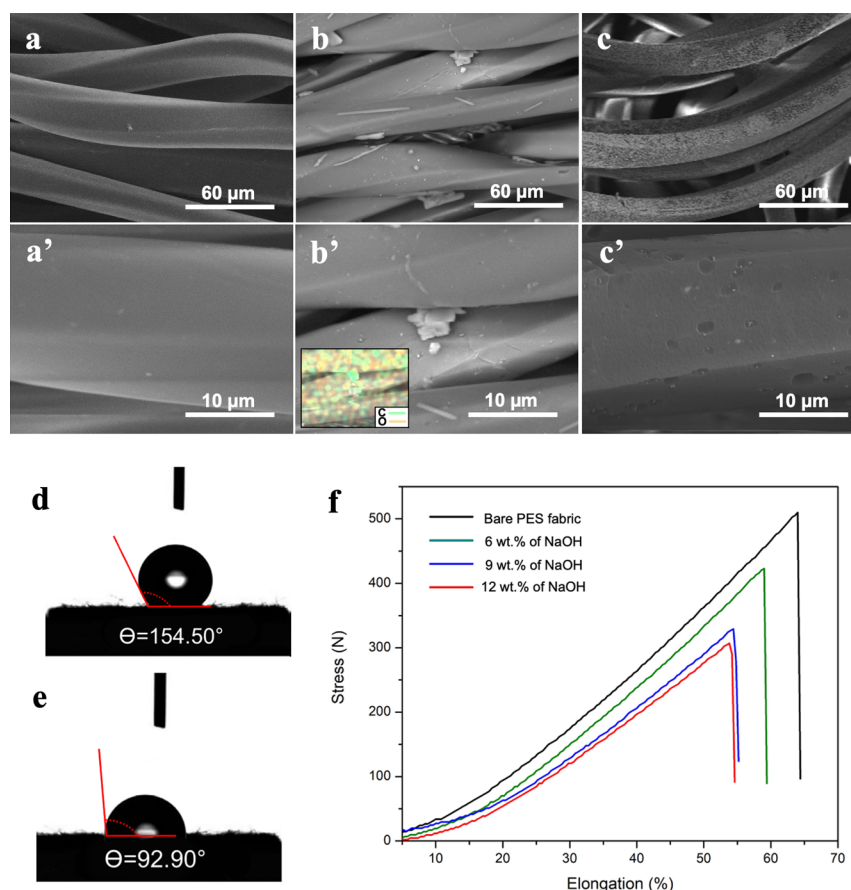


Figure 3. Surface morphology of (a, a') unhydrolyzed bare PES fabric and (b, b') hydrolyzed PES fabric amid alkaline hydrolysis. The inset image in b' exhibits the EDX mapping analysis of carbon (C) and oxygen (O). (c, c') Postalkaline treated hydrolyzed PES fabric at 300 \times and 800 \times magnifications, respectively. Photographs of the water contact angle of (d) unhydrolyzed PES fabric and (e) posthydrolyzed PES fabric. (f) Tensile stress of hydrolyzed PES fabrics in three concentrations of NaOH.

from 5.80 ± 2.59 to $64.46 \pm 2.22\%$ upon treatment with 0 to 12 wt %, respectively. This trend later remains relatively constant at $\sim 55\%$ when being hydrolyzed by more than 12 wt % of NaOH (Figure 2d). The fabric that was hydrolyzed with 12% NaOH showed the highest water absorption rate at 64.46%. Notably, the rise in the water absorptivity rate can be attributed to the elimination of oil and wax from fabric fibers.

Furthermore, the fabric's hydrophilicity was expected to improve upon NaOH hydrolyzation as this treatment stimulated the expansion of the hydrophilic surface. Meanwhile, hydrolyzed PES fabrics with 15% NaOH absorbed roughly 7% less water than its 12% NaOH counterpart. The absorption rate increased to approximately 44.70% when the NaOH concentration was 21%. A slight decrease in the water absorption rate took place when the fabric was hydrolyzed with more than 12% NaOH. This finding could be pointed to the excessive removal of the polar group in PES, which was detrimental to the fibers and subsequently caused a dip in water absorption.⁴⁵ Getnet and Chavan found that 15–30% PES weight loss due to alkali treatment changed the fabric's physical properties, such as silky handle, luster, soil repellency, and antistatic properties.²⁵ Further investigations on the properties of fabrics with 6, 9, and 12% NaOH were performed.

The surface morphology of bare or unhydrolyzed PES fabrics was observed through SEM. The surface displayed significant changes after each stage of treatment; 3a, 3a' before,

3b, 3b' during, and 3c, 3c' posthydrolysis, as shown by SEM micrographs in Figure 3. The bare fabric that underwent the hydrolysis in 12 wt % of NaOH (optimum condition) was used in this analysis. The bare fabric exhibited a smooth and clear surface structure. During treatment, small pieces of fibers were observed on the surface, suggesting detachment from the fabric substrate. EDX mapping in the inset of Figure 3b' reveals that carbon (C) was the primary element in the pieces. This proof of carbon indicated the removal of terephthalates such as oil and waxy components. In posthydrolysis treatment in Figure 3c,c', the formations of voids with accompanying increases in surface porosity of the hydrolyzed fabric were observed. The removal of PES terephthalate coating generated an uneven surface of PES due to the separation of carbonyl and hydroxyl groups from the ester group as described in the FTIR analysis. These circumstances possibly modified the structure of the fiber surface, which invariably influenced its hydrophilicity.

The hydrophilicity of hydrolyzed fabrics was further examined by assessing their wettability behavior with contact angle analysis. The contact angles of water droplets on unhydrolyzed and hydrolyzed PES fabrics are compared and shown in Figure 3d,e, respectively. PES is well known as a natural polymeric material that is hydrophobic, at $\sim 154.50^\circ$ absorption angle (as measured on unhydrolyzed PES fabrics).⁴⁶ The contact angle of water on hydrolyzed PES fabrics was 92.90° . This angle equated to a 61.60% reduction in the contact angle compared to unhydrolyzed fabrics. This

finding suggested that the PES fabric was successfully treated to enhance its hydrophilic properties. The consequences of contact angle analysis were in accordance with the discoveries of water absorption rate and weight loss rate analyses.

The mechanical properties of hydrolyzed PES fabrics at various alkali concentrations were demonstrated via the tensile stress test, as shown in Figure 3f. At the same time, the breaking force data is tabulated in Table 1. The tensile stress of

Table 1. Tensile Stress and Elongation Rate of Each Fabric

hydrolyzed PES fabric	tensile stress (N)	elongation rate (%)
bare PES fabric	520	64.5
6 wt % of NaOH	425	59.9
9 wt % of NaOH	328	55.0
12 wt % of NaOH	305	54.8

unhydrolyzed PES fabrics was treated as the control with a 520 N breaking force and 64.5% elongation rate. In this study, an increase in the concentration of hydrolysis was observed to couple with a decrease in the fabric's tensile stress. The tensile stress of 6% hydrolyzed PES dropped dramatically to 425 N breaking force.

The breaking force of the treated PES fabric was 18% lower than the breaking force of the unhydrolyzed fabric, indicating a deterioration of treated fibers. The breaking force plunged further to 328 and 305 N when the treatment concentration was raised to 9 and 12%, respectively. This decrease in breaking force could be linked to a lack of strong bonding between the fibers and the breaking of their mechanical connection.⁴⁷ Simultaneously, the elongation rate of the fabrics dropped steadily with increasing hydrolysis from 64.5 to 54.8%. The weak adhesion between the core level and the fiber surface could be the source of this trend. Although the mechanical properties displayed a deteriorating trend, PES fabrics with 9 and 12% NaOH had minuscule differences between each other, which offered an indicator for an optimum treatment concentration.

The surface morphology of PANI coating on hydrolyzed PES fabrics is depicted in Figure 4. As discussed in previous sections, the surface morphology of the bare PES fabric transformed after thermochemical treatment. PANI-coated unhydrolyzed PES in Figure 4a,a' shows an even surface

morphology compared to coarse and uncompact appearance with partially covered by some aggregations. Meanwhile, PANI-coated hydrolyzed fabrics in Figure 4b,b' shows a higher aggregation of PANI particles that implied rough surface adhesion. This occurrence encouraged electrical conductivity as the fibers were completely coated with the conductive network.

The DG conveys the percentage of PANI diffusion on hydrolyzed fabrics. Figure 4c shows the effect of hydrolyzed fabrics at various hydrolysis concentrations on the DG of PANI, while the DG of PANI is tabulated in Table 2. The DG

Table 2. DG of PANI in Various Concentrations of Hydrolyzed PES Fabrics

hydrolyzed PES fabric (wt %)	DG of PANI (%)
0 (bare/unhydrolyzed)	12.62 ± 0.72
3	16.58 ± 0.44
6	23.89 ± 0.52
9	30.96 ± 0.13
12	36.25 ± 0.60
15	36.18 ± 0.91
18	35.34 ± 0.60
21	36.16 ± 0.73

of PANI in the hydrolyzed PES fabric increased linearly with PES hydrolysis concentration from 0 to 12 wt %. The maximum DG was 36.25 ± 0.60 wt %, which was higher than the reported DG of Anbarasan et al.⁴⁸ and Wu et al.,¹⁸ (Table 3). During this phase, the absorption capacity of PANI was

Table 3. Comparison of the DG of PANI into Fabrics

no.	DG of PANI into fabrics	reference
1.	~9 wt %	48
2.	~20 wt %	18
3.	~36.25 wt %	this study

optimized in core yarns, which correlated to the SEM images in Figure 4b,b'. The PANI precipitate filled the void and pores in the hydrolyzed PES fabric. A further increase in the concentration of the hydrolyzed fabric to 21 wt % produced a significant plunge in the DG. It could be speculated that PANI

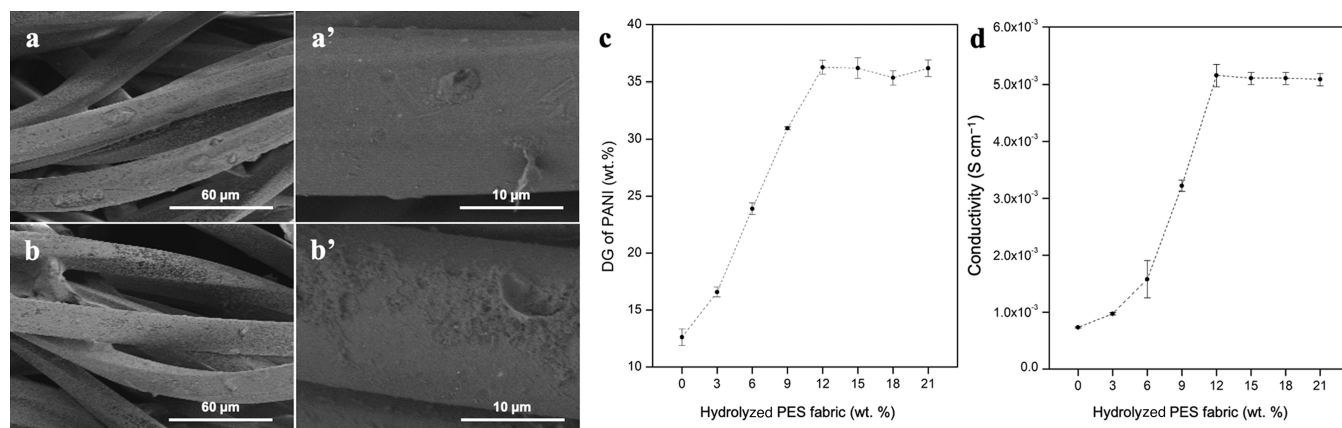


Figure 4. Surface morphology (a, a') of the PANI-coated unhydrolyzed PES fabric and (b, b') PANI-coated hydrolyzed PES fabric via immersion at 300× and 800× magnifications, respectively. (c) Effect of the hydrolyzed fabric at various hydrolysis concentrations on the DG of PANI. (d) Conductivity of PANI-hydrolyzed PES fabrics at various hydrolysis concentrations.

had reached its maximum absorption rate at this point, which deterred the interdiffusion of PANI into the fibers.⁴⁹ The results of DG against hydrolyzed PES in various hydrolysis concentrations reflected a similar trend with the water absorption rate of hydrolyzed PES fabrics as discussed previously. Collectively, the findings demonstrated that the thermochemical path is a highly effective approach to graft PANI onto fabrics.

The conductivity of PANI-coated hydrolyzed PES fabrics in various hydrolysis concentrations showed similar growth trends as the effect of the DG of PANI (Figure 4d). The conductivity of each hydrolyzed fabric is listed in Table 4. The

Table 4. Conductivity of Hydrolyzed PANI Fabrics in Various Hydrolysis Concentrations

hydrolyzed PES fabric (wt %)	conductivity ($S\text{ cm}^{-1}$)
0 (bare/unhydrolyzed)	$7.32 \pm 0.15 \times 10^{-4}$
3	$9.73 \pm 0.08 \times 10^{-4}$
6	$1.58 \pm 0.87 \times 10^{-4}$
9	$3.22 \pm 0.01 \times 10^{-4}$
12	$5.15 \pm 0.29 \times 10^{-4}$
15	$5.10 \pm 0.01 \times 10^{-4}$
18	$5.10 \pm 0.01 \times 10^{-4}$
21	$5.08 \pm 0.04 \times 10^{-4}$

12 wt % hydrolyzed fabric showed the highest conductivity value of $5.15 \pm 0.29 \times 10^{-3} S\text{ cm}^{-1}$ due to the excellent conductive network of PANI on the fabric. There were no

significant changes in the conductivity value when the hydrolysis concentration exceeded 12%. Therefore, the 12% hydrolyzed PANI fabric and unhydrolyzed PANI fabric were selected as samples for the washing durability test.

As seen in Figure 5, the conductivity value of unhydrolyzed PANI was reduced by three orders of magnitudes after 10 washing cycles (Table 5). This conductivity decay implied the

Table 5. Changes in Conductivity of Unhydrolyzed and Hydrolyzed PANI Fabrics in Each Washing Cycle

washing cycle	conductivity ($S\text{ cm}^{-1}$)	
	unhydrolyzed PANI fabric	hydrolyzed PANI fabric
0	$3.30 \pm 0.01 \times 10^{-3}$	$5.15 \pm 0.29 \times 10^{-3}$
1	$8.43 \pm 0.26 \times 10^{-4}$	$4.22 \pm 0.01 \times 10^{-3}$
2	$6.50 \pm 0.05 \times 10^{-4}$	$4.10 \pm 0.07 \times 10^{-3}$
3	$4.10 \pm 0.04 \times 10^{-4}$	$3.92 \pm 0.05 \times 10^{-3}$
4	$8.30 \pm 0.02 \times 10^{-5}$	$3.80 \pm 0.10 \times 10^{-3}$
5	$4.33 \pm 0.06 \times 10^{-5}$	$3.75 \pm 0.04 \times 10^{-3}$
6	$3.40 \pm 0.02 \times 10^{-5}$	$3.70 \pm 0.05 \times 10^{-3}$
7	$7.30 \pm 0.02 \times 10^{-6}$	$3.69 \pm 0.03 \times 10^{-3}$
8	$5.65 \pm 0.06 \times 10^{-6}$	$3.68 \pm 0.01 \times 10^{-3}$
9	$5.15 \pm 0.07 \times 10^{-6}$	$3.66 \pm 0.04 \times 10^{-3}$
10	$3.22 \pm 0.01 \times 10^{-6}$	$3.65 \pm 0.03 \times 10^{-3}$

weak durability of PANI fabrics.¹⁸ A significant drop in conductivity was discovered after the fourth washing cycle (from $3.30 \pm 0.01 \times 10^{-3}$ to $8.30 \pm 0.02 \times 10^{-5} S\text{ cm}^{-1}$). This

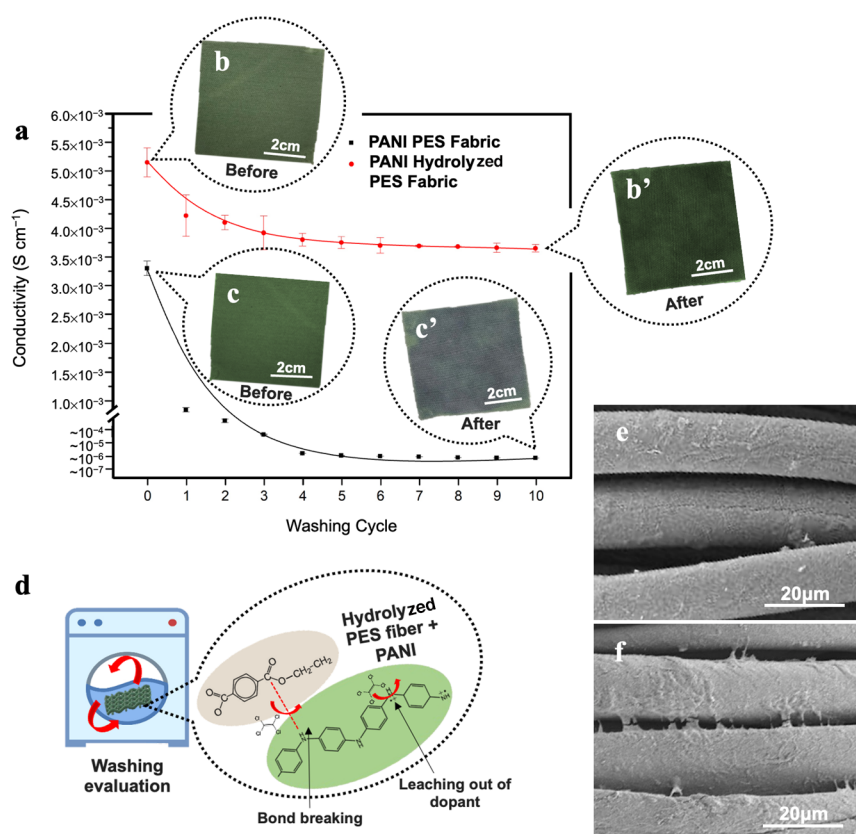


Figure 5. (a) Electrical conductivity of hydrolyzed and unhydrolyzed PANI fabrics in each washing cycle. Visual appearances in (b, b') represent the hydrolyzed PANI fabric, while (c, c') represent the unhydrolyzed PANI fabric before and after washing. (d) Illustration of washing evaluation on PANI fabrics and their plausible reactions. The postwashing SEM micrographs of (e) unhydrolyzed PANI fabric and (f) hydrolyzed PANI fabric at 500X magnification.

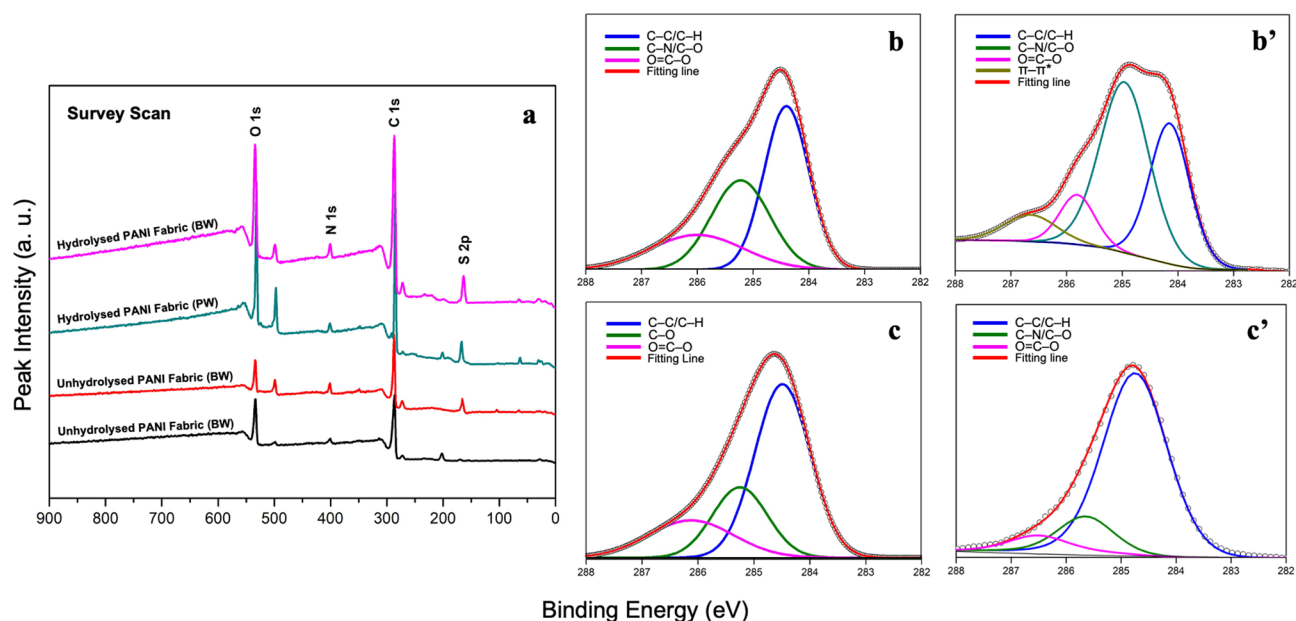


Figure 6. (a) Survey scan spectra of before (BW) and postwashed (PW) hydrolyzed and unhydrolyzed PANI fabrics. The BW and PW C 1s core spectra of (b, b') hydrolyzed PANI fabric and (c, c') unhydrolyzed PANI fabric.

conductivity depreciation could be attributed to the leaching of PANI and dopants from the fabric. The mechanical actions of scouring damaged the PANI coatings on the fabric. In addition, the hydrogen bond breaking between the fabric and PANI preceded dopant discharge. The increased temperature during washing introduced kinetic energy that further weakened the bond.^{6,50} All of these circumstances led to the disintegration of PANI from the fabric.

From the fourth to tenth washing cycle, the conductivity remained constant in one order of magnitude between 10^{-5} and 10^{-6} S cm^{-1} . As shown in Figure 5a, the green appearance of the unhydrolyzed PANI fabric was a sign of its emeraldine salt state before the washing test. At this state, PANI was conductive. After 10 washing cycles, the PANI fabric exhibited slight visual changes to a nonuniform distribution of greenish-blue color (Figure 5a'). The transition from green to blue was characteristic of PANI's switch from conductive to non-conductive. The unhydrolyzed PANI fabric had poor durability after 10 washing cycles.

Furthermore, its conductivity values entered the insulator phase with three magnitudes of decrement.¹⁴ Since conductivity was consistent under the fourth cycle, the washing test was terminated at the tenth cycle. Interestingly, the conductivity of the hydrolyzed PANI fabric remained at a similar order of magnitude ($\sim 10^{-3}$ S cm^{-1}) throughout all washing cycles. The thermochemical treatment of the PES fabric improved the ability of the conductive network to withstand the washing process. This evidence underlined the credibility of PANI chemical grafting to produce conductive fabrics with stable electrical characteristics. Furthermore, hydrolyzed PES fabrics encouraged maximum integration of PANI within the fibers by offering greater surface adhesion. In the long run, this optimized integration would prolong the lifespan of conductive fabrics. As shown in Figure 5b,b', the lack of color changes in the fabrics alluded to the status quo of PANI's conductive emeraldine salt state after the washing test.

Figure 5e shows SEM micrographs of postwashed unhydrolyzed and hydrolyzed PANI fabrics. The surface of

the unhydrolyzed PANI fabric exhibited cracks. The cracks were caused by the removal of PANI coating from the fabric due to mechanical scrubbing and scouring during washing (as illustrated in Figure 5d). Furthermore, factors like bond breaking due to weak surface adhesion between PANI and the dopant could lead to disintegration and deprotonation of the conductive network from the fabric. These combined actions played a role in conductivity depreciation. In contrast, the homogenous surface of hydrolyzed PANI fabrics in Figure 5f showed better fiber integrity with intact PANI coating on the fabric after the washing test. Therefore, it was proven that thermochemical treatment could reinforce the durability and electrical functionality of PANI by modifying the surface structure of the PES fabric.

The washing test was valuable in understanding the durability of hydrolyzed and unhydrolyzed PANI fabrics with respect to their conductivity value. After 10 washing cycles, it was believed that PANI had leached from the fabric, which compromised its electrical integrity. Hence, quantifying the postwashing chemical composition or changes in PANI's protonation level provided more significant insights into the fabric's lifespan. XPS analysis was employed to quantify these changes. The survey scan spectra in Figure 6a provides an overall composition in the fabric; oxygen (O 1s \sim 532 eV), nitrogen (N 1s \sim 400 eV), carbon (C 1s \sim 285 eV), and sulfur (S 2p \sim 168 eV).

The primary elements of C 1s, N 1s, O 1s, and S 2p have been scrutinized at high energy resolution. High-resolution C 1s spectra of the fabrics are presented in Figure 6b,b',c,c', which revealed four prominent peaks at \sim 284.51, \sim 285.42, \sim 286.31, and \sim 286.93 eV. These peaks were attributed to C-C/C-H, C-N/C-O, O=C-O groups, and π - π^* , respectively. Waware et al. discovered that the C-C group corresponded to the polymer backbone, thus validating the finding of this study.⁵¹ In the fitted peaks of Figure 6b, the decreasing relative intensity of C-C/C-H in the hydrolyzed PANI fabric was noted, while the intensity of two peaks (C-O and O=C-O) rose significantly. This outcome demonstrated

the modification of oxygen-containing polar functional groups during the thermochemical treatment. According to Krylova et al., these groups are primarily responsible for enhanced wettability and grafted PANI in hydrolyzed PANI fabrics.⁵² A lower composition of the polar functional group is observed compared to unhydrolyzed PANI fabrics in Figure 6c. The shake-up satellite ($\pi-\pi^*$) could be observed due to the excessive interaction of photoelectrons.⁵³ The area of high-resolution spectra was measured to determine the elemental compositions in BW and PW hydrolyzed and unhydrolyzed PANI fabrics (Table 6).

Table 6. Elemental Compositions of BW and PW Hydrolyzed and Unhydrolyzed PANI Fabrics

fabric	condition	C (%)	N (%)	O (%)	S (%)
hydrolyzed PANI fabric	BW	48.94	15.6	29.13	6.33
	PW	63.46	10.30	21.12	5.12
unhydrolyzed PANI fabric	BW	65.39	12.30	18.11	4.20
	PW	80.58	5.10	13.22	1.10

The sulfur content of BW hydrolyzed and unhydrolyzed PANI fabrics were 6.33 and 4.20%, respectively, according to the S 2*p* core line spectra. As informed from N 1*s* spectra, nitrogen content was 15.60 and 12.30% for BW hydrolyzed and unhydrolyzed PANI fabrics, respectively. However, there were slips in element composition after the washing test. According to Mahat et al., these depreciations were caused by the depletion of the dopant groups ($-\text{SO}_3^-$) and PANI ($-\text{NH}_2-$) from the surface.⁴⁵ An increase in carbon composition (C 1*s*) could compensate for the loss of the dopant in the PANI backbone. Further details on the oxidation state change of N 1*s* and S 2*p* spectra are described in the following section.

The N 1*s* core level spectra shown in Figure 7a,b were used to track the chemical changes in hydrolyzed and unhydrolyzed

PANI fabrics while simultaneously observing protonation changes in the polymer backbone. Due to the varying chemical conditions, these spectra could be placed under four distinct chemical states; imine ($=\text{N}-$) at 398.5 eV, amine ($-\text{NH}-$) at 399.5 eV, protonated amine ($-\text{NH}_2^+$) at 401.1 eV, and protonated imine ($=\text{NH}^+$) at 402.2 eV. After the washing test, both hydrolyzed and unhydrolyzed PANI fabrics displayed a decrease in peak intensity in protonated amine and imine groups, as seen in Figure 7a',b'. The drop in doping levels indicated nitrogen elimination, which is similar to polaron/bipolaron. The deprotonation level of N^+ species was calculated for overall nitrogen content (Table 7).

Postwashed unhydrolyzed PANI fabrics exhibited deprotonation levels of 36.99 and 26.61% due to the migration of tiny anion dopants from the fabric during washing and their extended cycles. The diffusion of dopant fragments and their loss preceded this deprotonation. Therefore, this confirms our earlier explanation that some of the *p*TSA-PANI structures had contributed to breaking up its chain and leaching out from the fabric substrate during the washing obstacle. The deprotonation of PANI led to a reduced-salt form and loss of electrical conductivity. In contrast, the hydrolyzed PANI fabric slightly dropped its deprotonation level from 44.77 to 42.68%. This distinct value (compared to the unhydrolyzed PANI fabric) confirmed that the hydrolyzed PANI fabric had managed to preserve protonated species of nitrogen contents after the washing test. Moreover, this phenomenon suggests that the novel thermochemical treatment that employed in hydrolyzed fabrics proves to enhance the durability behavior of PANI in the fabrics and maintain the longevity of its electrical functionalities.

Cifarelli et al. found that the diffusion of tiny dopant anions from the PANI fabric could justify the deprotonation mechanism.⁵⁴ Therefore, further quantification of sulfur content is a viable technique to expose the disintegration of dopants. The sulfur content in BW and PW hydrolyzed and

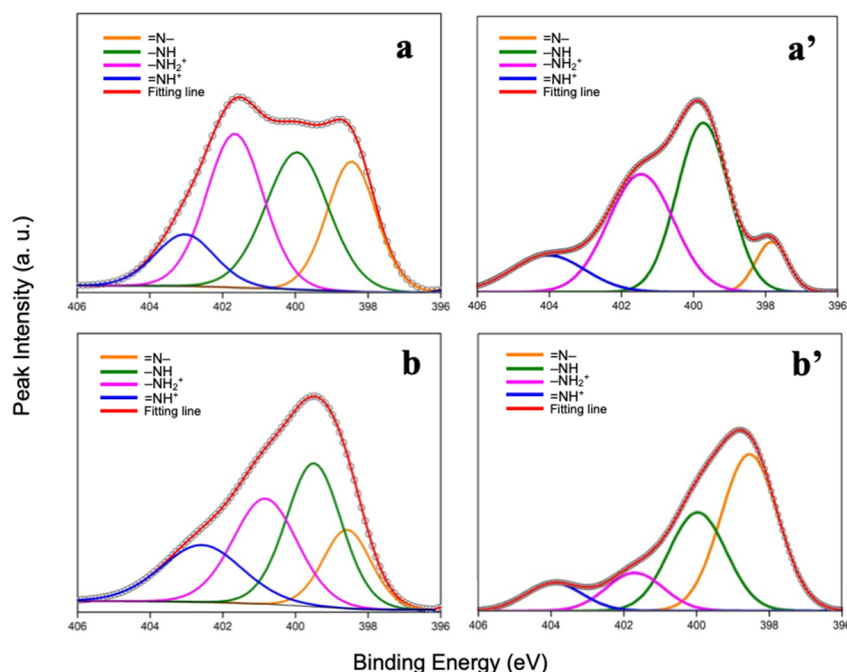


Figure 7. N 1*s* core level spectra: (a, a') hydrolyzed PANI fabric and (b, b') evaluation of before (BW) and postwashed (PW) unhydrolyzed PANI fabric, respectively.

Table 7. Ratio of Nitrogen Species to Total Nitrogen Content of BW and PW Hydrolyzed and Unhydrolyzed PANI Fabrics

fabric	condition	imine (=N–)	amine (NH–)	protonated imine (NH ₂ ⁺)	protonated amine (=NH ⁺)	level of doping (%)
unhydrolyzed PANI fabric	BW	0.36	0.27	0.19	0.18	36.99
	PW	0.38	0.35	0.15	0.12	26.61
hydrolyzed PANI fabric	BW	0.29	0.26	0.25	0.20	44.77
	PW	0.15	0.42	0.24	0.19	42.68

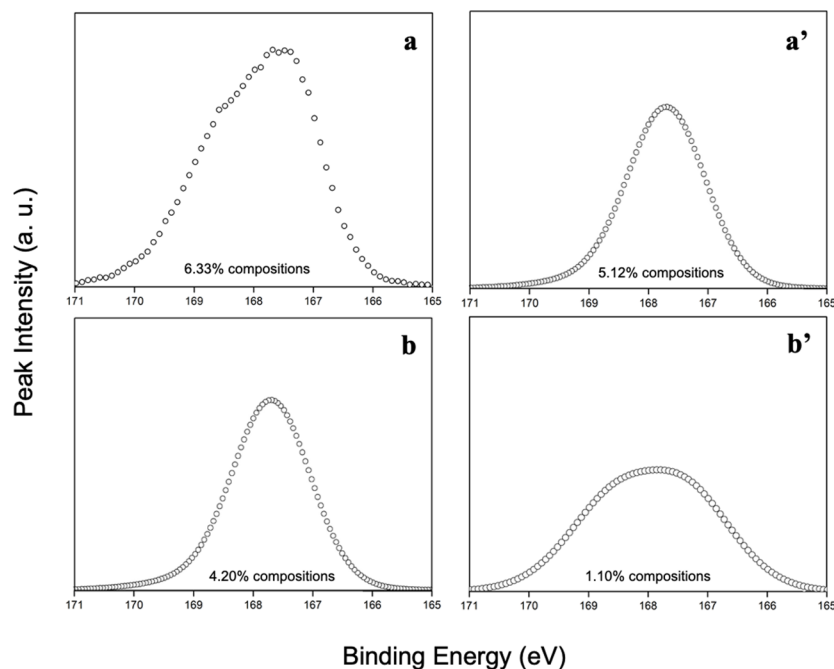


Figure 8. S 2p core line spectra of the dopant fragment in (a, a') hydrolyzed PANI fabric and (b, b') BW and PW unhydrolyzed PANI fabric, respectively.

unhydrolyzed PANI fabrics were quantified through the S 2p core line spectra, as visualized in Figure 8a,b, respectively. It described the sulfur in ring-attached monosubstituents like SO₃ and SO₃H at a binding energy of ~168.00 eV.⁵⁵ Positively charged nitrogen (NH²⁺) in doped PANI fabrics suggested an electrostatic interaction with dopant anions (SO₄²⁻).⁵⁶ Hydrolyzed PANI fabrics (Figure 8a) had significantly retained their dopant compositions after washing (Figure 8a'). After washing, a minor depreciation from 6.33 to 5.12% of total sulfate species was observed. The presence of this element on postwashed PANI validated the improvement of its stability that provided better surface attachment in PANI-hydrolyzed fabrics, which explains the key to the longevity in electrical functionality. Comparing to the unhydrolyzed PANI fabric (Figure 8a'), the higher drop of total sulfate species from 4.20 to 1.10% exhibits weaker stability of dopant fragments with the PANI host in postwashing (Figure 8b').

CONCLUSIONS

We demonstrate the fabrication of conductive PANI integrated onto a PES substrate to address the challenge of poor durability and conductivity of conductive fabrics during the washing test, where the leaching of the dopant could be observed. The fabric's color from green (conductive state) to blue has been devised into a nonconductive form and faded. The conductivity of the PANI fabric was reduced by three orders of magnitudes from $3.30 \pm 0.01 \times 10^{-3}$ to $3.22 \pm 0.01 \times 10^{-6}$ S cm⁻¹ due to leaching of dopants from the fabrics. This drawback could hinder the fabrics' functionality in field

applications, such as wearable bioelectronics. Here, the novel thermochemical treatment was employed to the polyester fabric. Consequently, the climbing PANI DG was found from 12.62% (unhydrolyzed fabric) to 36.25% (hydrolyzed fabric), which suggested an improved adhesion between PANI and the fabric. Contact angle analysis resulted in a significant 61.60% reduction, confirming the successful enhancement of the fabric's hydrophilic properties. Additionally, the conductivity of the hydrolyzed PANI fabric remained stable at a magnitude of 10⁻³ S cm⁻¹ after 10 washing cycles, demonstrating improved durability compared to the unhydrolyzed fabric (which experienced a drop by three orders of magnitude). Furthermore, investigation using XPS through N 1s core line spectra revealed that the hydrolyzed PANI fabric preserved its deprotonation level from 10.38 to 2.09% after washing, indicating better retention of its electrical properties compared to the unhydrolyzed fabric. The thermochemical treatment of the PES fabric improved the durability of the conductive network when the fabric was washed. Therefore, it was proven that the grafting of PANI onto the fabric is a valid means to prepare a conductive fabric with stable electrical characteristics.

ASSOCIATED CONTENT

Supporting Information

The Supporting Information is available free of charge at <https://pubs.acs.org/doi/10.1021/acsomega.3c03377>.

Enhancing the washing durability and electrical longevity of conductive polyaniline grafted polyester fabric (PDF)

AUTHOR INFORMATION

Corresponding Author

Mohd Muzamir Mahat – School of Physics and Material Studies, Faculty of Applied Sciences and Textile Research Group, Faculty of Applied Sciences, Universiti Teknologi MARA, 40450 Shah Alam, Malaysia; orcid.org/0000-0002-2448-3241; Phone: +60193364616; Email: mmuzamir@uitm.edu.my

Author

Muhammad Faiz Aizamddin – School of Physics and Material Studies, Faculty of Applied Sciences, Universiti Teknologi MARA, 40450 Shah Alam, Malaysia

Complete contact information is available at:

<https://pubs.acs.org/10.1021/acsomega.3c03377>

Author Contributions

All authors have given approval to the final version of the manuscript.

Notes

The authors declare no competing financial interest.

ACKNOWLEDGMENTS

The authors gratefully acknowledge financial support from Universiti Teknologi MARA (UiTM), Malaysia: 600-RMC/GPK 5/3 (177/2020)—Revealing the Mechanism of Electronic Conduction of Polyaniline Fabrics by XPS.

REFERENCES

- (1) Aizamddin, M. F.; Mahat, M. M.; Nawawi, M. A.; Jani, N. A.; Ariffin, Z. Z.; Yahya, S. Y. S. Electrical conductivity and thermal stability of conductive polyaniline fabric-based polyacrylonitrile blends. *AIP Conf. Proc.* **2023**, *2720*, No. 040020.
- (2) Sedighi, A.; Montazer, M.; Mazinani, S. Fabrication of electrically conductive superparamagnetic fabric with microwave attenuation, antibacterial properties and uv protection using PEDOT/magnetite nanoparticles. *Mater. Des.* **2018**, *160*, 34–47.
- (3) Gong, Y.; Fu, K.; Xu, S.; Dai, J.; Hamann, T. R.; Zhang, L.; Hitz, G. T.; Fu, Z.; Ma, Z.; Mcowen, D. W.; Han, X.; Hu, L.; Wachsmann, E. D. Lithium-ion conductive ceramic textile: A new architecture for flexible solid-state lithium metal batteries. *Mater. Today* **2018**, *21*, 594–601.
- (4) Omar, S. N. I.; Ariffin, Z. Z.; Zakaria, A.; Safian, M. F.; Halim, M. I. A.; Ramli, R.; Sofian, Z. M.; Zulkifli, M. F.; Aizamddin, M. F.; Mahat, M. M. Electrically conductive fabric coated with polyaniline: Physicochemical characterisation and antibacterial assessment. *Emergent Mater.* **2020**, *3*, 469–477.
- (5) Biermaier, C.; Bechtold, T.; Pham, T. Towards the functional ageing of electrically conductive and sensing textiles: A review. *Sensors* **2021**, *21*, 5944.
- (6) Ismar, E.; Kurşun Bahadır, S.; Kalaoglu, F.; Koncar, V. Futuristic clothes: Electronic textiles and wearable technologies. *Glob. Chall.* **2020**, *4*, No. 1900092.
- (7) Sundriyal, P.; Bhattacharya, S. Textile-based supercapacitors for flexible and wearable electronic applications. *Sci. Rep.* **2020**, *10*, 13259.
- (8) Zhang, Y.; Wang, H.; Lu, H.; Li, S.; Zhang, Y. Electronic fibers and textiles: Recent progress and perspective. *iScience* **2021**, *24*, No. 102716.
- (9) Aizamddin, M. F.; Shafiee, S. N. A.; Halizan, M. Z. M.; Shafiee, S. A.; Sabere, A. S. M.; Sofian, Z. M.; Daud, N.; Bahrudin, F. I.; Harun, I.; Rahman, N. A.; Mahat, M. M. Utilizing membrane technologies in advancing the recycling of spent lithium-ion batteries using green electrochemical method – A review. *Mater. Res. Proc.* **2023**, *29*, 170–191.
- (10) Aizamddin, M. F.; Mahat, M. M.; Roslan, N. C.; Adila, D.; Ruzaidi, A.; Ayub, A. N. Techniques for designing patterned conducting polymers. In *Conjugated Polymers For Next Generation Applications*; Woodhead Publishing: 2022, *1*, 39–77.
- (11) Roslan, N. C.; Aizamddin, M. F.; Adila, D.; Ruzaidi, A.; Ayub, A. N.; Ain, N.; Asri, N.; Jani, N. A.; Shafiee, S. A.; Mahat, M. M. 10. Conducting Polymer-Based Textile Materials. In *Conjugated Polymers For Next Generation Applications*; Woodhead Publishing: 2022, *1*, 325–359.
- (12) Shahemi, N. H.; Mahat, M. M.; Asri, N. A. N.; Amir, M. A.; Ab Rahim, S.; Kasri, M. A. Application of Conductive Hydrogels on Spinal Cord Injury Repair: A Review. *ACS Biomater. Sci. Eng.* **2023**, *9*, 4045–4085.
- (13) Ayub, A. N.; Ismail, N. A.; Aizamddin, M. F.; Bonnia, N. N.; Sulaiman, N. S.; Nadzri, N. I. M.; Mahat, M. M. Effects of Organic Solvent Doping on the Structural and Conductivity Properties of PEDOT: PSS Fabric. *J. Phys.: Conf. Ser.* **2022**, *2169*, No. 012008.
- (14) Tomczykowa, M.; Plonska-Brzezinska, M. E. Conducting polymers, hydrogels and their composites: Preparation, properties and bioapplications. *Polymers (Basel)* **2019**, *11*, 350.
- (15) Mahat, M. M.; Mawad, D.; Nelson, G. W.; Fearn, S.; Palgrave, R. G.; Payne, D. J.; Stevens, M. M. Elucidating the deprotonation of polyaniline films by X-ray photoelectron spectroscopy. *J. Mater. Chem. C* **2015**, *3*, 7180–7186.
- (16) Stamminger, R.; Bues, A.; Alfieri, F.; Cordella, M. Durability of washing machines under real life conditions: Definition and application of a testing procedure. *J. Clean. Prod.* **2020**, *261*, No. 121222.
- (17) Cui, J.; Zhou, S. Highly conductive and ultra-durable electronic textiles via covalent immobilization of carbon nanomaterials on cotton fabric. *J. Mater. Chem. C* **2018**, *6*, 12273–12282.
- (18) Wu, B.; Zhang, B.; Wu, J.; Wang, Z.; Ma, H.; Yu, M.; Li, L.; Li, J. Electrical switchability and dry-wash durability of conductive textiles. *Sci. Rep.* **2015**, *5*, 11255.
- (19) Arora, R.; Singh, N.; Balasubramanian, K.; Alegaonkar, P. Electroless nickel coated nano-clay for electrolytic removal of Hg(II) ions. *RSC Adv.* **2014**, *4*, 50614–50623.
- (20) Huang, D.; Zheng, Q.; Guo, K.; Chen, X. Wearable supercapacitor based on polyaniline supported by graphene coated polyester textile. *Int. J. Energy Res.* **2021**, *45*, 21403–21413.
- (21) Palacios-Mateo, C.; van der Meer, Y.; Seide, G. Analysis of the polyester clothing value chain to identify key intervention points for sustainability. *Environ. Sci. Eur.* **2021**, *33*, 2.
- (22) Gao, A.; Shen, H.; Zhang, H.; Feng, G.; Xie, K. Hydrophilic modification of polyester fabric by synergetic effect of biological enzymolysis and non-ionic surfactant, and applications in cleaner production. *J. Clean. Prod.* **2017**, *164*, 277–287.
- (23) Karimah, A.; Ridho, M. R.; Munawar, S. S.; Adi, D. S.; Ismadi; Damayanti, R.; Subiyanto, B.; Fatriasari, W.; Fudholi, A. A review on natural fibers for development of eco-friendly bio-composite: Characteristics, and utilizations. *J. Mater. Res. Technol.* **2021**, *13*, 2442–2458.
- (24) Musale, R. M.; Shukla, S. R. Weight reduction of polyester fabric using sodium hydroxide solutions with additives cetyltrimethylammonium bromide and [BMIM]Cl. *J. Text. Inst.* **2017**, *108*, 467–471.
- (25) Getnet, M.; Chavan, R. Catalyzation of alkaline hydrolysis of polyester by oxidizing agents for surface modification. *Int. J. Sci. Basic Appl. Res.* **2015**, *22*, 232–252.
- (26) Xiong, S.; Wang, R.; Zhang, X.; Wu, Y.; Xu, Z.; Ma, B.; Zhang, X.; Qu, Q.; Wu, B.; Chu, J.; Wang, X.; Zhang, R.; Gong, M.; Chen, Z. Covalent bonding of PANI and p-phenylenediamine-functionalized GO using N,N'-Dicyclohexylcarbodiimide as dehydrating agent for electrochromic applications. *Chem. Sel.* **2019**, *4*, 543–550.
- (27) Mahat, M. M.; Aizamddin, M. F.; Roslan, N. C.; Kamarudin, M. A.; Nurzatul, S.; Omar, I.; Mazo, M. M. Conductivity, morphology and thermal studies of polyaniline fabrics. *Aust. J. Mech. Eng.* **2020**, *9*, 137–150.

- (28) Aizamddin, M. F.; Mahat, M. M.; Ariffin, Z. Z.; Nawawi, M. A.; Jani, N. A.; Amdan, N. A. N.; Sadasivuni, K. K. Antibacterial performance of protonated polyaniline-integrated polyester fabrics. *Polymers (Basel)* **2022**, *14*, 2617.
- (29) Aizamddin, M. F.; Roslan, N. C.; Kamarudin, M. A.; Omar, S. N. I.; Safian, M. F.; Halim, M. I. A.; Mahat, M. M. Study of conductivity and thermal properties of polyaniline doped with p-toluene sulfonic acid. *Malaysian J. Anal. Sci.* **2020**, *24*, 413–421.
- (30) Aizamddin, M. F.; Mahat, M. M.; Nawawi, M. A. Morphological, structural and electrochemical studies of conductive polyaniline coated polyester fabrics. *Proc. Int. Exc. Inn. Conf. Eng. Sci.* **2019**, 53–57.
- (31) Wang, S.; Wang, Z.; Li, J.; Li, L.; Hu, W. Surface-grafting polymers: From chemistry to organic electronics. *Mater. Chem. Front.* **2020**, *4*, 692–714.
- (32) Maity, N.; Dawn, A. Conducting polymer grafting: Recent and key developments. *Polymer* **2020**, *12*, 709.
- (33) Aizamddin, M. F.; Mahat, M. M.; Ariffin, Z. Z.; Samsudin, I.; Razali, M. S. M.; Amir, M. A. Synthesis, characterisation and antibacterial properties of silicone–silver thin film for the potential of medical device applications. *Polymers (Basel)* **2021**, *13*, 3822.
- (34) Gleissner, C.; Landsiedel, J.; Bechtold, T.; Pham, T. Surface activation of high performance polymer fibers: A review. *Polym. Rev.* **2022**, *62*, 757–788.
- (35) Zhao, X.; Xiong, M.; Jiang, L.; Yang, Q.; Zhou, C.; Liu, J. The effect of washing parameters on the quantity of dye discharge from clothes. *Fash. Text.* **2022**, *9*, 13.
- (36) Kawai, F.; Kawase, T.; Shiono, T.; Urakawa, H.; Sukigara, S.; Tu, C.; Yamamoto, M. Enzymatic hydrophilization of polyester fabrics using a recombinant cutinase cut 190 and their surface characterization. *J. Fiber Sci. Technol.* **2017**, *73*, 8–18.
- (37) Fockaert, L. I.; Pletincx, S.; Ganzinga-Jurg, D.; Boelen, B.; Hauffman, T.; Terryn, H.; Mol, J. M. C. Chemisorption of polyester coatings on zirconium-based conversion coated multi-metal substrates and their stability in aqueous environment. *Appl. Surf. Sci.* **2020**, *508*, No. 144771.
- (38) Zhang, Y.; Shahid-ul-Islam; Rather, L. J.; Li, Q. Recent advances in the surface modification strategies to improve functional finishing of cotton with natural colourants - A review. *J. Clean. Prod.* **2022**, *335*, No. 130313.
- (39) Rahman, R.; Gul, A.; Lensen, M. C.; Akhter, Z. Ferrocene-based polyesters with azobenzene linker: synthesis and biological evaluation. **2022**, DOI: 10.21203/rs.3.rs-2051814/v1.
- (40) Mountaki, S. A.; Kaliva, M.; Loukelis, K.; Chatzinikolaïdou, M.; Vamvakaki, M. Responsive polyesters with alkene and carboxylic acid side-groups for tissue engineering applications. *Polymers (Basel)* **2021**, *13*, 1636.
- (41) Ćorak, I.; Tarbuk, A.; Đorđević, D.; Višić, K.; Botteri, L. Sustainable alkaline hydrolysis of polyester fabric at low temperature. *Materials (Basel)* **2022**, *15*, 1530.
- (42) Dhinakaran, M.; Dasaradan, B. S.; Subramaniam, V. A new method of investigating the structure by weight loss of polyester fibers. *J. Text. Appar. Technol. Manag.* **2010**, *6*, 1–8.
- (43) Dhakal, H. N.; Zhang, Z. Y.; Richardson, M. O. W. Effect of water absorption on the mechanical properties of hemp fibre reinforced unsaturated polyester composites. *Compos. Sci. Technol.* **2007**, *67*, 1674–1683.
- (44) Mittal, M.; Chaudhary, R. Experimental study on the water absorption and surface characteristics of alkali treated pineapple leaf fibre and coconut husk fibre. *Int. J. Appl. Eng. Res.* **2018**, *13*, 12237–12243.
- (45) Muhammad, A.; Rashidi, A. R.; Wahit, M. U.; Sanusi, S. N. A.; Iziuna, S.; Jamaludin, S. Alkaline treatment on kenaf fiber to be incorporated in unsaturated polyester. *J. Eng. Appl. Sci.* **2016**, *11*, 11894–11897.
- (46) Azeem, M.; Wiener, J.; Khan, M. Z. Hydrophobic analysis of nano-filament polyester fabric. *Fibres Text.* **2018**, *25*, 5.
- (47) Huang, S.; Fu, Q.; Yan, L.; Kasal, B. Characterization of interfacial properties between fibre and polymer matrix in composite materials – A critical review. *J. Mater. Res. Technol.* **2021**, *13*, 1441–1484.
- (48) Anbarasan, R.; Muthumani, N.; Vasudevan, T.; Gopalan, A.; Wen, T. C. Chemical grafting of polyaniline onto nylon66 fiber in different media. *J. Appl. Polym. Sci.* **2001**, *79*, 1283–1296.
- (49) Hirn, U.; Schennach, R. Comprehensive analysis of individual pulp fiber bonds quantifies the mechanisms of fiber bonding in paper. *Sci. Rep.* **2015**, *5*, 10503.
- (50) Eaves, J. D.; Loparo, J. J.; Fecko, C. J.; Roberts, S. T.; Tokmakoff, A.; Geissler, P. L. Hydrogen bonds in liquid water are broken only fleetingly. *Proc. Natl. Acad. Sci. U. S. A.* **2005**, *102*, 13019–13022.
- (51) Waware, U. S.; Arukula, R.; Hamouda, A. M. S.; Kasak, P. Electrochemical and X-ray photoelectron spectroscopic investigations of conductive polymers. *Ionics* **2020**, *26*, 831–838.
- (52) Krylova, V.; Dukštienė, N.; Lelis, M.; Tučkutė, S. PES/PVC textile surface modification by thermo-chemical treatment for improving its hydrophilicity. *Surf. Interfaces* **2021**, *25*, No. 101184.
- (53) Mayer, D.; Lever, F.; Picconi, D.; Metje, J.; Alisauskas, S.; Calegari, F.; Düsterer, S.; Ehlert, C.; Feifel, R.; Niebuhr, M.; Manschwetus, B.; Kuhlmann, M.; Mazza, T.; Robinson, M. S.; Squibb, R. J.; Trabattoni, A.; Wallner, M.; Saalfrank, P.; Wolf, T. J. A.; Gühr, M. Following excited-state chemical shifts in molecular ultrafast X-ray photoelectron spectroscopy. *Nat. Commun.* **2022**, *13*, 198.
- (54) Cifarelli, A.; Berzina, T.; Parisini, A.; Iannotta, S. Memristive Response and electrochemical processes in polyaniline based organic devices. *Org. Electron.* **2020**, *83*, No. 105757.
- (55) Siow, K. S.; Britcher, L.; Kumar, S.; Griesser, H. J. XPS study of sulfur and phosphorus compounds with different oxidation states. *Sains Malays.* **2018**, *47*, 1913–1922.
- (56) Hwang, D. K.; Song, D. M.; Im, S. S. Synthesis of villi-structured polyaniline sheets using organic single crystal surface-induced polymerization. *ACS Omega* **2018**, *3*, 4181–4186.